[19]C. D. Zerby, Oak Ridge National Laboratory Report ORNL-3033, 1961 (unpublished).
[20]J. W. Motz and R. C. Placious, Phys. Rev. 109, 235 (1958).
[21]J. W. Motz, Phys. Rev. 100, 1560 (1955).
[22]M. Scheer, E. Trott, and G. Zahs, Z. Physik 209, 68 (1968).
[23]C. Fronsdal and H. Überall, Phys. Rev. 111, 580 (1958).
[24]J. W. Motz and R. C. Placious, Nuovo Cimento 15, 571 (1960).
[25]R. L. Gluckstern and M. H. Hull, Phys. Rev. 90, 1030 (1953).

PHYSICAL REVIEW VOLUME 180, NUMBER 1 5 APRIL 1969

Electron-Impact Excitation and Negative-Ion Formation in NH_3 and ND_3†

R. N. Compton, J. A. Stockdale, and P. W. Reinhardt

Health Physics Division, Oak Ridge National Laboratory, Oak Ridge, Tennessee 37830
(Received 28 October 1968)

Threshold electron-impact excitation of ammonia has been studied using both "trapped electron" and "SF_6 electron-scavenger" techniques. Results from the two excitation studies show four well-defined peaks in the energy range from 6 to 12 eV. The scavenger spectrum exhibits a small peak below the first singlet state which is analogous to that previously found for H_2O and is tentatively attributed to a triplet state. Also, an intense peak is observed at approximately 17 eV. Dissociative electron-capture cross sections for NH_3 and ND_3 have been measured with a total ionization chamber and the various ions contributing to these cross sections were recorded as functions of the electron energy with a TOF mass spectrometer using electron beams with resolution of ~0.1 eV. The total negative-ion cross section for NH_3 (5.74×10^{-18} cm^2) peaking at 5.65 eV is approximately 1.1 times larger than the ND_3 cross section (5.36×10^{-18} cm^2) peaking at 5.86 eV which is analogous to previous results for water and heavy water. The total ionization cross section for ND_3 peaked at ~0.21-eV higher energy than that for NH_3. This is ascribed to a difference in the zero-point energy for the two molecules. The electron energy scale determined from Cl^-/HCl in the mass-spectrometer study of the various ion-current peaks (e.g., H^-, NH_2^-, NH^-, etc.) corresponded exactly to that obtained for the cross sections using the 19.31-eV He^- resonance in the total ionization measurements. Accurate measurements of the H^- (D^-) ion kinetic energy as a function of incident electron energy yield a dissociation energy of 4.35 ± 0.15 eV for NH_2-H (or ND_2-D).

I. INTRODUCTION

Two basic classes of experiments have evolved for studying electronic excitation of molecules by electron impact. The first is designed to determine the energy distribution of the inelastically scattered electrons for a fixed-energy incident beam. The scattered electron energy distributions are referred to as "energy-loss spectra." The spectra are usually detected for forward scattering although angular distributions are presently being studied. In the second type of scattering experiment a nearly monoenergetic electron beam of variable mean energy is directed into a gas, and only those electrons having lost essentially all of their energy upon collision are detected. In this case, total collection of "zero-energy" electrons is carried out, independent of the scattering direction. Since the incident electron energy must exactly match the excitation threshold of the target molecule before a scattered current is measured (i.e., completely inelastic collision), the spectrum obtained is referred to as a "threshold excitation spectrum." At present there are two basic experiments used to study threshold excitation: (1) the trapped-electron technique and (2) the more recent electron-scavenger method.

In 1958 Schulz[1] introduced the trapped-electron method in which low-energy electrons resulting from inelastic scattering are trapped in a shallow

electrostatic well (~ 0.1 – 0.2 eV) introduced into the scattering chamber. Since only electrons having lost nearly all of their energy are collected, the incident energy must closely match the excitation potential of the molecule before a trapped-electron current is detected. The resulting plot of current versus electron energy is a threshold electron-impact excitation spectrum. Contributions to the measured trapped-electron current may also arise due to elastic scattering (especially at low energies) and to the formation of negative ions which must be considered in an analysis of the data. Details of the construction and operating potentials of the trapped-electron apparatus have been discussed by Schulz.[1,2]

The recent SF_6 scavenger technique first demonstrated by Curran[3] is a very sensitive method of detecting optically forbidden transitions by electron impact. This method utilizes the intense resonance electron attachment process in SF_6 at ~0.0 eV to scavenge electrons which have suffered inelastic collisions with a sample gas in a mass spectrometer. Electrons with energy very close to the excitation threshold of a molecule AB are "thermalized" to ~ 0.0 eV by a single inelastic-scattering event and subsequently captured by SF_6. The sequential reactions can be written

$$e_{\text{fast}} + AB \rightarrow AB^* + e_{\text{thermal}}, \qquad e_{\text{thermal}} + SF_6 \rightarrow SF_6^- . \tag{1}$$

A plot of the SF_6^- ion current versus incident electron energy obtained in this manner is therefore a threshold excitation spectrum. The method is especially useful for the detection of optically forbidden transitions because such transitions are allowed under electron impact and often the excitation functions are strongly peaked near threshold. The SF_6 scavenger technique has several distinct advantages for the study of electronic excitation at threshold. For instance, negative ions produced in the collision chamber by electron collisions with the sample gas do not contribute to the SF_6^- signal but can be analyzed separately, whereas such ions often contribute to the current of the trapped-electron technique. The simultaneous detection of a precisely known negative-ion process can oftentimes be used as a means of calibrating the electron energy scale. Also, no electrostatic potential is imposed into the collision chamber avoiding any effect on the mean energy or width of the electron beam.

Recently, dissociative attachment processes in molecules have been the subject of a considerable number of theoretical and experimental studies. An excellent review of the present state of the theory has been presented by J. C. Y. Chen.[4] Experimental investigations of capture cross sections for H_2,[5,6] H_2O,[7] CH_4,[8] and the hydrogen halides[9] (and their deuterated analogs) together with studies of temperature effects upon dissociative attachment cross sections[10] have provided quantitative tests for much of the theory. *A priori* calculations of electron-attachment cross sections and subsequent isotope effects are not possible at this stage, and the need for experimental studies in this field remains evident.

In this paper we present experimental studies of threshold electron-impact excitation and negative-ion formation in ammonia and deuterated ammonia. To our knowledge only two other electron-impact excitation studies of ammonia have been performed[11,12] (incident electron energies from 33 to 300 V), and no threshold excitation studies have been reported. Dissociative electron attachment in ammonia has been studied by a number of authors[13–17]; however, only the most recent study[16] has presented cross-section data. Data are presented also on the cross sections for dissociative electron attachment, negative-ion yields as a function of energy, and kinetic energies of the product ions for NH_3 and ND_3.

II. EXPERIMENTAL

The "SF_6 electron-scavenger" technique previously employed by Compton *et al.*[18] was modified to incorporate automatic retarding potential-difference techniques. A Bendix TOF mass spectrometer identical to that previously described[19] was employed. The electron beam was gated on for ~ 5 μsec intervals at a repetition rate of 15 kHz, corresponding to a rectified electron current of ~ 10^{-8} A. A square wave or sinusoidal modulation signal of ~ 0.1-V amplitude was applied to the retarder grid of the electron gun at a frequency of 22 Hz. Thus electrons within the modulated band which take part in dissociative attachment or become scavenged through process (1) produce ion currents which are modulated at the same frequency. Following amplification by an electron multiplier and electrometer, the fraction of the ion current produced by electrons in the ~ 0.10-V band was obtained by demodulation of the ion currents at a frequency of 22 Hz with a "lock-in" amplifier. The ion mass being monitored could be selected within the range 1 – 300 amu with a resolution of better than 1 amu. Ion currents were recorded as a function of electron energy on an X-Y plotter. The X axis displacement was synchronized with the motor driven potentiometer that continuously varied the electron energy through a selected range. The electron energy scale in these mass spectrometer studies was calibrated by use of the Cl^-/HCl dissociative attachment resonance.[18]

In the second type of scattering experiment, trapped-electron spectra, dissociative attachment

cross sections, and ion kinetic energies were determined from the cylindrical electron collision apparatus shown in Fig. 1. Dimensions of the apparatus are given in the caption to the figure. The collision chamber and inner gold grid were held at ground potential. The outer grid and total ionization collector were tied together electrically. Saturation of the electron current to the electron collector was achieved with an electric field of only a few volts/cm. Saturation of the negative-ion current to the ion collector required an electric field of 6.5 V/cm. Quasimonoenergetic electron beams with resolution of ~0.1 eV were produced in the manner described in the TOF mass spectrometer experiments above. The trapped electron and negative-ion currents were recorded as continuous functions of the electron energy on an X-Y recorder. The well depth in the trapped-electron studies was estimated by observing the shift in the resonance state in nitrogen at 11.87 eV[20] as a function of the potential producing the field penetration into the collision region.

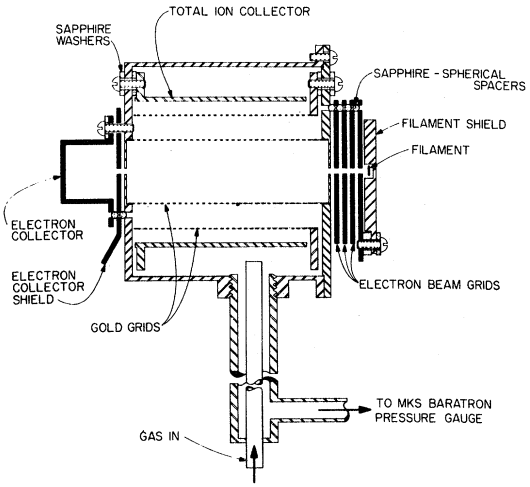

FIG. 1. Diagram of electron collision chamber. Collision-chamber path length = 1.515 in. Diameter of ion collector = 1.15 in. Electron-beam apertures in electron-beam grids are 30 mil holes, exit to electron collector is 40 mil hole. Background pressures were generally less than 1×10^{-8} Torr.

The electron energy scale and electron energy resolution were determined by observing the transmission resonance in helium at 19.31 eV.[21] The width of the He^- resonance at one-half of its maximum value was 0.15 eV which is an indication of the electron energy resolution. The electron energy resolution (i.e., observed width of the He^- resonance) did not change noticeably upon addition of ammonia. The peak in the He^- resonance, which was used to set the electron energy scale, could be read to within 0.05 eV. Zero suppression of the transmitted current in the region of the He^- resonance permitted the use of a relatively small helium pressure ($\sim 10^{-4} - 10^{-3}$ mm Hg) for the calibration runs. Calibration of the electron energy scale by the He^- resonance is superior to observing the trapped-electron peak resulting from the $He(2^3S)$ state since this state can be excited with electron energies greater than its threshold (19.81 eV). Consequently, the accuracy of the electron energy scale calibrated by the $He(2^3S)$ level is attended by an uncertainty as large as the well depth ($\sim 0.1 - 0.3$ eV).

Gas pressures in both the mass spectrometer and total ionization chamber were determined with an M.K.S. Baratron capacitance manometer employing a "1-Torr" head. The accuracy of the pressure measurements in the mass spectrometer has been discussed previously[22] and is believed to be ±10%. The accuracy of the pressure measurements (and other systematic errors) for the total ionization experiment was checked by determining the cross section for dissociative electron attachment in oxygen. The maximum O^-/O_2 cross section was determined to be 1.6×10^{-18} cm^2 which is in excellent agreement with previous values. Thus the pressure measurements in the two experiments are believed to be accurate to within 10%.

III. THRESHOLD EXCITATION SPECTRA OF AMMONIA

The "SF_6 scavenger" threshold excitation spectrum of ammonia is presented in Fig. 2. The electron energy scale was calibrated by use of the NH_2^- peak at 5.65 eV (See Sec. V). The horizontal bars (indicating the wavelength range of the observed transitions) and the electronic state designations shown in Fig. 2 are taken from the compilation by Herzberg.[23] The arrows (↓) designate energy-loss peaks observed by Skerbele and Lassettre[11] for 300-eV incident energy electrons. The peak in the region from 6 to 7 eV is attributed to excitation of the lowest optically allowed state of ammonia ($^1A_2''$). The peak is slightly skewed toward lower energies which may be due to charge exchange between H^- or NH_2^- and SF_6. The peak at ~8.6 eV does not correlate well with either the optically observed states or the energy-loss peaks of Skerbele and Lassettre.[11] It is reasonable to ascribe the peak in the region from 10 to 11 eV to the $\tilde{G}$ state. The structure in the peak around 12 eV is due to noise. The center of the peak correlates with a small peak in the high-energy data of Skerbele and Lassettre; however, due to the difference in incident electron energy the two states may not be the same.

A small peak below the first singlet ($^1A_2''$) state with a maximum at ~4.4 eV is reproducible in the SF_6 scavenger spectrum for ammonia. A similar

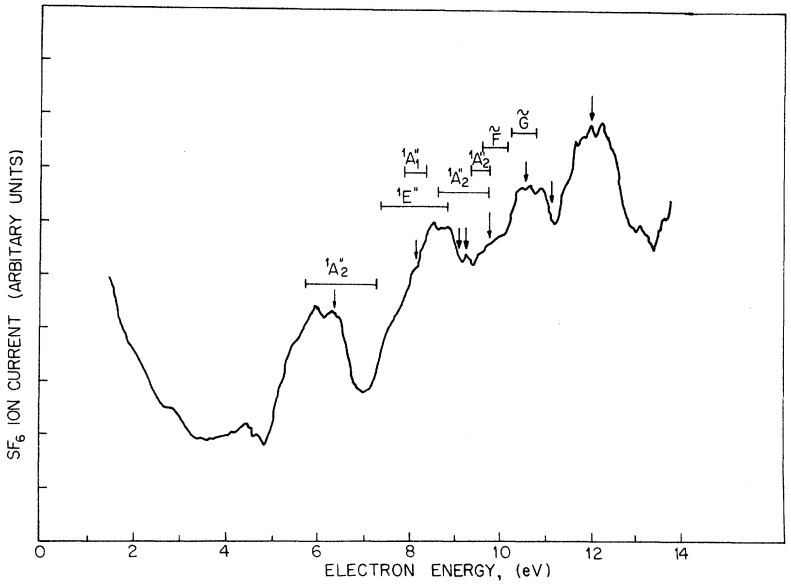

FIG. 2. "SF_6 scavenger" threshold electron-impact excitation spectrum of ammonia.

structure was observed in the excitation spectrum obtained for water vapor by Schulz[24] (trapped electron) and Compton *et al.*[18] (SF_6 scavenger) and was tentatively attributed to a triplet state although the possibility of a transient negative-ion state giving rise to this peak was not ruled out. The existence of this state has been confirmed more recently by Skerbele, Dillon, and Lassettre[25] who observed electron energy losses from electrons of 30-to 60-eV incident energy. Thus transient negative-ion formation is not responsible for the low-energy peak in water vapor, which leaves a triplet state as the most plausible explanation. By analogy with the water vapor results, we suggest that the peak in ammonia at ~ 4.4 eV is due to a low-lying triplet state. Excitation of triplet states of ammonia by photon impact has not been reported. Thompson and Duncan[26] searched for optical transitions to the lowest triplet below 6.5 eV using an absorbing path length of 10 m with ammonia at 1 atm but were unable to detect any absorption.

The general rise in the SF_6^- current as the electron energy decreases below 3 eV is due to (1) the primary electron capture-resonance in SF_6 peaking at zero energy and (2) inelastic scattering in the low energy region. Since the electron energy resolution is generally ~ 0.1 to 0.3 eV, considerable inelastic scattering is believed to be occurring although no actual peak was observed for energies from 0 to 3 eV.

The "trapped-electron" spectrum of ammonia is shown in Fig. 3 for incident electron energies from

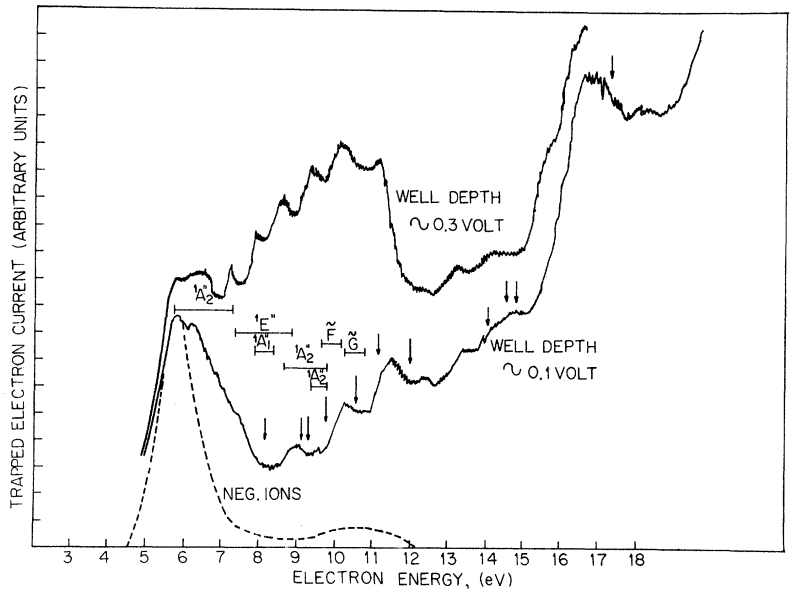

FIG. 3. "Trapped-electron" electron-impact excitation spectra of ammonia.

5 to 20 eV. Two different well depths (~0.1 and ~0.3) are represented. As in the scavenger spectrum, the horizontal bars and state designations are taken from Herzberg[23] and the arrows (↓) indicate energy loss peaks reported by Skerbele and Lassettre.[11] The large peak in the region from 5 to 8 eV is composed of both negative ions and inelastic electron scattering due to the $^1A_2''$ state. The dashed curve represents the negative-ion contribution to the "trapped-electron" current (recorded with approximately zero well depth). Using a well depth of ~0.1 eV, the $^1A_2''$ peak is slightly resolved from the negative-ion peak and a shoulder at ~7.5 eV hints at the possibility of another state in this energy region. It was not possible to observe the low energy (4.4-eV) peak which was detected in the scavenger spectrum due to the intense negative-ion current peak in this region.

The three major peaks in the region from 8.5 to 12 eV correspond to those of the scavenger spectrum; however, the peak energies are about 0.2 eV lower in energy. This is due in part to the difficulty in locating the peak energy of the negative-ion current in the 9 to 12-eV region, the intensity ratios of the three inelastic peaks are roughly the same as the corresponding peaks of the SF_6 scavenger spectrum. Thus the "SF_6 scavenger" data and "trapped-electron" spectrum for 0.1-V well depth are in fair agreement over the energy range from 5 to 12 eV. Peaks also occur above 12 eV and 12.3, 13.5, ~14.5, 16.8 (center of the broad maximum), and ~18 eV. A shoulder also occurs at ~16 eV. All of these peaks are also evident in the data using the deeper well (0.3 V). Sun and Weissler[27] have studied vacuum ultraviolet absorption cross sections in ammonia and find a weak maximum

$$\sigma = 21 \text{ Mb}, \quad \text{at } 1130 \pm 20 \text{ Å } (11.0 \pm 0.2 \text{ eV}),$$

and a strong maximum[26]

$$\sigma = 34 \text{ Mb}, \quad \text{at } 730 \pm 20 \text{ Å } (17 \pm 0.5 \text{ eV}).$$

The two maxima have been associated with the ionization limits of the outer electrons of ammonia. It is reasonable to suspect that the broad peak centered at ~16.8 eV corresponds to the strong absorption observed in the vacuum ultraviolet spectrum. Although ionization electrons probably contribute to the trapped-electron current around 16.8 eV, Metzger and Cook[28] have argued that processes other than ionization (e.g., dissociation) also occur between 13 and 17 eV. In view of the structure observed in the trapped-electron spectrum from 12 to 19 eV, this is most probably correct.

IV. CROSS SECTIONS FOR PRODUCTION OF NEGATIVE IONS

The dissociative attachment cross sections for ammonia and deuterated ammonia are shown in Fig. 4. The two curves represent ion currents as a function of electron energy under identical source conditions (pressure and electron current) with the ordinate adjusted to give the cross section for ammonia as measured according to the procedure outlined in Sec. II. Twenty-three measurements of the cross section for ammonia obtained at different pressures and after different gas fillings result in an average cross section of 5.74×10^{-18} cm^2 with a maximum deviation of $\pm 0.2 \times 10^{-18}$ cm^2 from this value. The average of 17 corresponding measurements for deuterated ammonia yielded an average cross

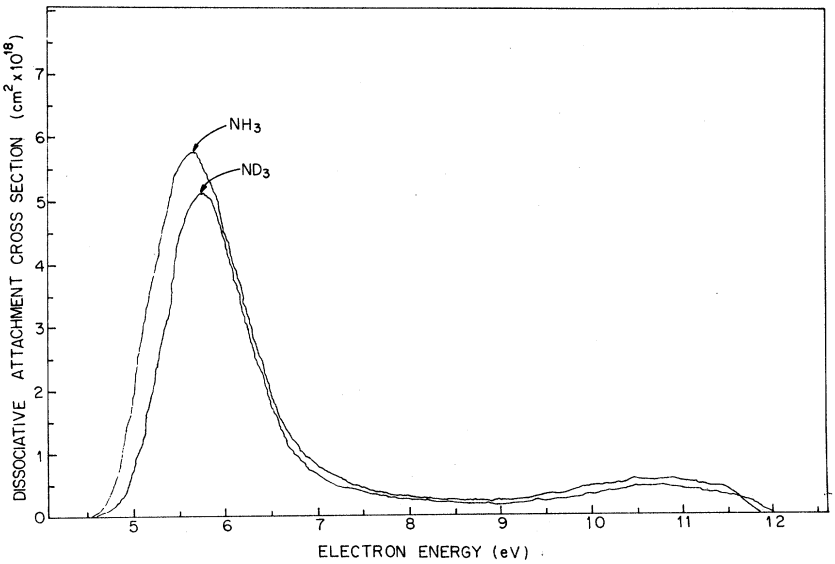

FIG. 4. Dissociative electron-attachment cross sections for ammonia and deuterated ammonia.

section of 5.36×10^{-18} cm^2 with a maximum deviation of $\pm0.3\times10^{-18}$ cm^2. The standard deviation for the ammonia cross-section measurements was 0.12×10^{-18} cm^2 and for ammonia $-d_3$ 0.22×10^{-18} cm^2. The dissociative attachment isotope effect determined from the peak values (at~5.7 eV) of the direct cross-section measurements is

$$\sigma_{NH_3}/\sigma_{ND_3}=\tfrac{5.74}{5.36}=1.07.$$

The isotope effect determined by negative-ion current measurements upon alternate gas fillings of NH_3 and ND_3 under identical source conditions gives

$$\sigma_{NH_3}/\sigma_{ND_3}=1.11.$$

The two ratios are in reasonable agreement; however, the latter measurements are believed to be more accurate since in these measurements the electron emission did not change upon adding gas to the system (the pressure in the electron filament region was always less than 1×10^{-6} mm Hg). The isotope effect determined here is in exact agreement with that obtained independently by Sharp and Dowell.[16]

The absolute cross-section measurement was checked for NH_3 by determining the negative-ion production-peak cross section relative to the positive ionization cross section at 85 eV. Reversing the ion collector field and appropriately adjusting the electron energy, the ratio of the negative-ion cross section to positive-ion cross section was 0.31 ± 0.002. The positive-ion cross sections for ammonia have been measured by a number of authors: 2.21 Å^2 (at 80 eV);[29] 3.54 Å^2 (at 75 eV);[30] 2.2 – 2.5 Å^2 (at 70 eV);[31] and 2.0 Å^2 (at 100 eV).[15] Multiplication of the average of these measurements (2.5 Å^2) by 0.031 gives a negative-ion cross section at the peak for ammonia of 7.7×10^{-18} cm^2. This is reasonably close to our directly measured value of 5.74×10^{-18} cm^2 and serves as a crude check of this value.

The effect of isotopic substitution upon the negative-ion cross sections for ammonia

$$(\sigma_{NH_3}/\sigma_{ND_3}=1.1)$$

is in the same direction but somewhat smaller than that previously found for water vapor[7]

$$(\sigma_{H_2O}/\sigma_{D_2O}=1.3).$$

The isotope effect observed for water vapor was accounted for in a quite straightforward manner by assuming that capture is possible due to the breakdown of the separation of nuclear and electronic motion in the Schrödinger equation, i.e., the nuclear kinetic-energy operator is the perturbation operator.[32] The ratio of the cross sections can be reduced to

$$\sigma_{NH_3}/\sigma_{ND_3}=(\mu_{D-ND_2}/\mu_{H-NH_2})^{1/2}\times\frac{|\langle\psi_f|\nabla^2R(H-NH_2)|\psi_i\rangle|^2}{|\langle\psi_f|\nabla^2R(D-ND_2)|\psi_i\rangle|^2}, \quad (2)$$

where ∇_R^2 represents the second derivative with respect to the distance separating the dissociating system [it will be shown later that for the peak in the cross section at ~5.6 eV only H^- (D^-) and NH_2^- (ND_2^-) need be considered], ψ_i and ψ_f are the initial and final nuclear wave functions. The simplest mass dependence on the peak cross section contained in the integrals represented in Eq. (2) is found by neglecting the final-state mass dependence and assuming that the square of the ground nuclear state wave function is projected upon a dissociating state in the Franck-Condon region. Under this assumption the ratio of the peak cross sections becomes

$$\left(\frac{\sigma_{NH_3}}{\sigma_{ND_3}}\right)_{peak}=\left(\frac{\mu_{D-ND_2}}{\mu_{H-NH_3}}\right)^{1/4}=1.21 \quad (3)$$

which is only slightly higher than the measured value. Thus it appears that the simplest interpretation of the isotope effects upon dissociative attachment in NH_3, H_2O,[7] HCl, HBr, and HI[9] arises from the kinetic-energy operator treatment. Autodetachment from the dissociating negative-ion system does not have to be invoked to explain these small direct isotope effects.

Calibration of the electron energy scale for the peaks in the electron-attachment cross sections shown in Fig. 4 was determined by observing the helium "window" at 19.31 eV and is believed accurate to within 0.05 eV. The peak in the ammonia-d_3 cross section peaked 0.21 eV at higher energy than the ammonia peak cross section. This difference in energy is surprisingly close to the difference in the total zero-point vibrational energies for these molecules (0.219 eV).

V. STUDY OF INDIVIDUAL IONS PRODUCED FROM NH_3 AND ND_3

The major dissociative attachment cross-section peak between 5 and 7 eV in NH_3 (ND_3) is composed of H^- (D^-) and NH_2^- (ND_2^-). Figure 5 shows a direct recorder trace of the ND_2^- current and a smooth line drawn through an average of three D^- tracings. The D^- current is seen to peak about

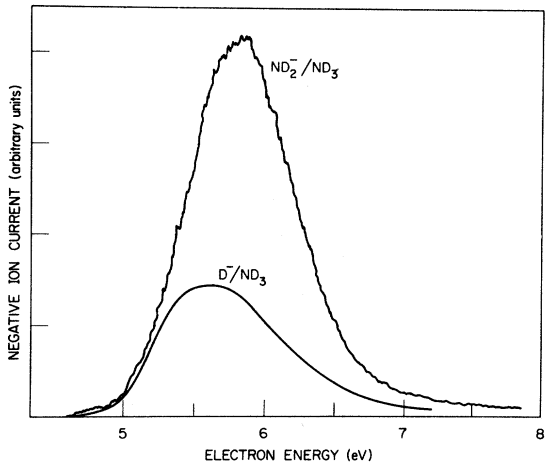

FIG. 5. Negative-ion current yields of D^- and ND_2^- from ND_3 as a function of electron energy.

0.2 eV lower in energy than ND_2^- (electron energy scale calibrated by Cl^-/HCl). The ratios of the D^- to ND_2^- intensities shown is probably too small because of ion discrimination in the mass-spectrometer source and because of a different initial multiplication factor at the electron multiplier. Similar curves were obtained for H^- and NH_2^- from NH_3.

The low-energy side of the NH_2^- peak is found to be broader than that of the rising part of the Cl^-/HCl curve indicating that NH_2^- is produced with a nonvertical onset. The energy at the peak NH_2^- (ND_2^-) as determined from the Cl^-/HCl calibration was 5.60(5.80) eV, which is in excellent agreement with the peak energies of the total ionization measurements calibrated by means of the 19.31-eV helium "window." Figure 6 shows direct recorder traces of NH_2^-, NDH^-, and ND_2^- currents with a mixture of NH_3 and ND_3 in the mass spectrometer. The NDH^- is present as a result of isotopic exchange between NH_3 and ND_3. Again one notices a 0.20 eV difference in the peak energies of NH_2^- and ND_2^- which is attributable to the zero-point energy difference in NH_3 and ND_3. As we would expect, NDH^- peaks midway between NH_2^- and ND_2^-.

The cross section for the production of ND_2^-/ND_3 was determined relative to the known cross section for O^-/N_2O, using the mass spectrometer. Since the ion kinetic energy and masses of these two ions (O^- and ND_2^-) are approximately the same, ion-current measurements at equal pressure mixtures of ND_3 and N_2O should be a reasonably good determination of the relative cross sections. The results gave

$$\sigma_{(ND_2^-/ND_3)} = 2.5 \pm 0.3 \times 10^{-18}\ \text{cm}^2,$$

using the cross section for O^-/N_2O as reported by Rapp and Briglia.[33] Sharp and Dowell[16] give

$$\sigma_{(D^-/ND_3)}/\sigma_{(ND_2^-/ND_3)} = 1.18,$$

which, combined with

$$\sigma_{(ND_2^-/ND_3)} = 2.5 \times 10^{-18}\ \text{cm}^2,$$

predict a total cross section of 5.4×10^{-18} cm^2 which is in excellent agreement with our directly measured value of 5.36×10^{-18} cm^2.

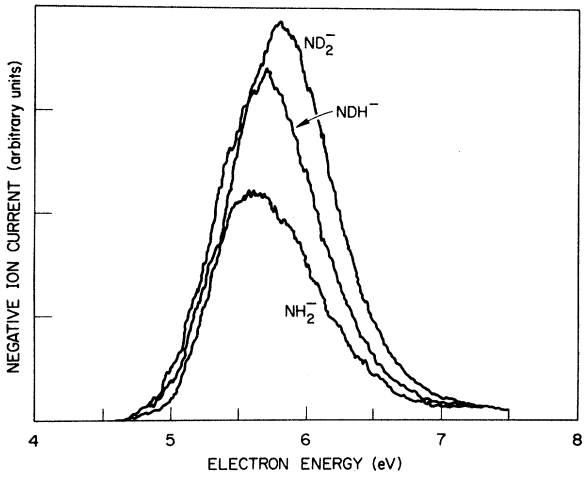

FIG. 6. Comparison of energy dependence of NH_2^- from NH_3 and ND_2^- from ND_3. NDH^- comes from NHD_2 and NDH_2 and is a result of isotopic exchange between NH_3 and ND_3.

Figure 7 shows NH_2^-, NH^-, and ND_2^-, ND^- ion currents in the electron energy range from 4 to ~14 eV. The ratio of the ND_2^- peak height at ~10 eV to that near 6 eV is 0.038; the corresponding ratio for the NH_2^- peaks is 0.029. The traces of Fig. 7 are normalized to equal NH_2^- and ND_2^- (see Fig. 5) peak heights at ~6 eV. The deuterated peaks (ND_2^- and ND^-) shown in Fig. 7 both occur at ~0.4-eV higher energy than the corresponding NH_2^- and NH^- peaks. This difference cannot be completely accounted for by the zero-point motion discussed in connection with the ~6-eV peaks.

Ion kinetic-energy measurements as a function of electron energy have been made for H^-/NH_3 and D^-/ND_3 in the energy region of 5 to 7 eV[34] by retarding the ion current reaching the ion collector. The automatic retarding potential-difference technique was employed to obtain electron energy resolution of ~0.1 eV. The retarding voltage required to reduce the ion current to zero was taken to be the ion kinetic energy for ions which enter the cylindrical retarding field at zero angle with respect to the field lines. Negative-ion currents from ND_3 are shown as a function of the continuously variable ion retarding voltage in Fig. 8

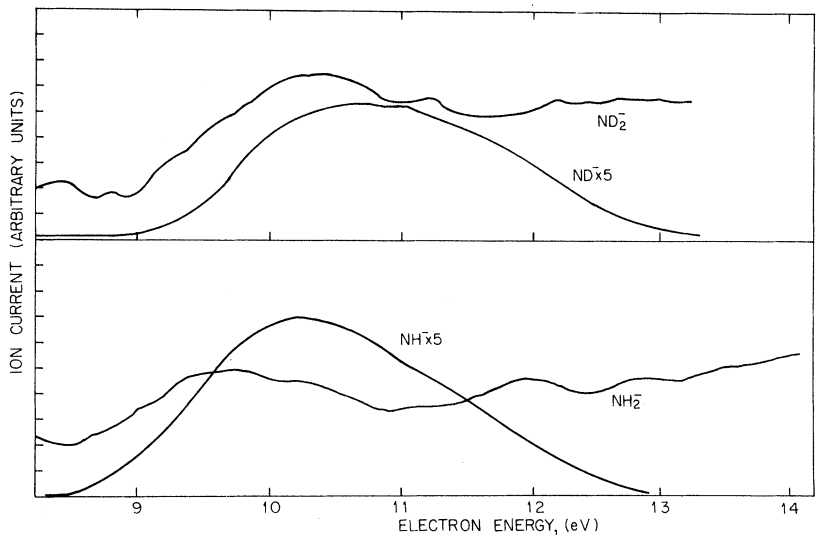

FIG. 7. Negative-ion current yields of ND^- and ND_2^- from ND_3 (NH_2^- and NH^- from NH_3) as a function of electron energy from ~9 – 14 eV.

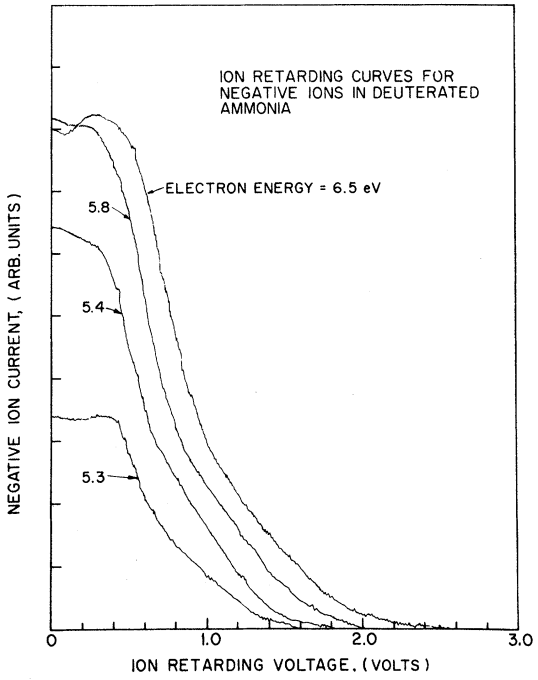

FIG. 8. Ion-retarding curves for negative ions in deuterated ammonia.

for various incident electron energies. The H^- and D^- ions will be the most energetic and correspond to the ions being the last to be retarded to zero energy as the retarding voltage is increased. For diatomic-like dissociations (i.e., the dissociation products are not vibrationally or rotationally excited), a plot of ion kinetic energy (E_i) versus electron energy (E_e) should follow the relationship

$$E_i = \left(1 - \frac{M_H}{M_{NH_3}}\right)\left[E_e - \left(D_{(NH_2 - H)} - E_{A(H)}\right)\right], \quad (4)$$

where M_H is the proton mass, M_{NH_3} the mass of ammonia, $D_{(NH_2 - H)}$ is the dissociation energy of the $NH_2 - H$ bond, and $E_{A(H)}$ is the electron affinity of the hydrogen atom. Figure 9 shows ion kinetic-energy plots versus electron energy for D^-/ND_3 and H^-/NH_3. Lines drawn through the points have the proper slope (0.90 for H^-/NH_3

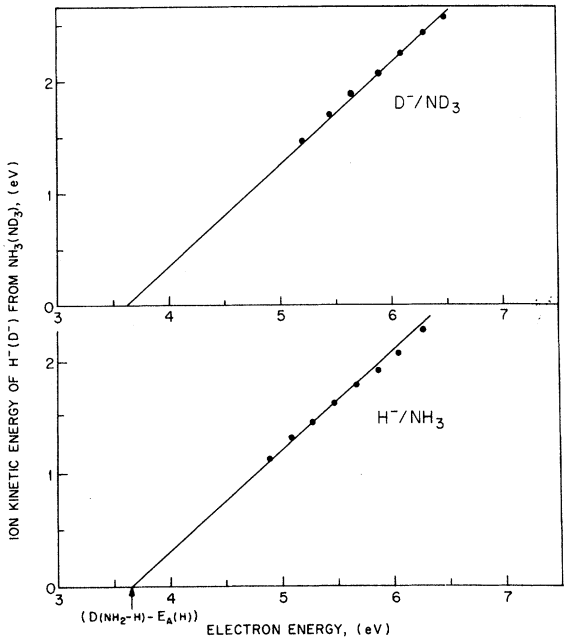

FIG. 9. Plot of ion kinetic energy as a function of electron energy for D^- from ND_3 and H^- from NH_3.

TABLE I. Dissociation energy of NH_2-H.

$D_{(NH_2-H)}$ (kcal/mole)	Method	Reference
< 124	predissociation	a
< 112	mercury photosensitization	b
< 117	fluorescence	c
104	$NH_3 + H = NH_2 + H_2$	d
104 ± 2	pyrolysis of hydrazine	e
100	pyrolysis of benzylamine	d
102	magnetron	f
106 ± 3	$e + NH_3 \rightarrow NH_2^+ + H + e$	g
100 ± 3	$e + NH_3 \rightarrow NH_2 + H^-$	h

[a]K. F. Bonhoeffer and L. Farkas, Z. Physik. Chem. A134, 337 (1928).

[b]H. W. Melville, Proc. Roy. Soc. (London) A152, 325 (1935).

[c]A. Terenin, J. Chem. Phys. 3, 436 (1935).

[d]M. Szwarc, Proc. Roy. Soc. (London) A198, 285 (1949).

[e]M. Szwarc, Proc. Roy. Soc. (London) A198, 267 (1949).

[f]F. M. Page, Trans. Faraday Soc. 57, 1254 (1961).

[g]S. N. Foner and R. L. Hudson, J. Chem. Phys. 29, 442 (1958).

[h]Present work.

and 0.94 for D^-/ND_3) and extrapolation to zero ion kinetic energy together with the known electron affinity of hydrogen yields a dissociation energy of 4.35 ± 0.15 eV (100 ± 3 kcal/mole) for NH_2-H or ND_2-D.[35] Table I compares this value with that determined by different techniques and good agreement is seen among the various methods.

ACKNOWLEDGMENTS

The authors are indebted to J. T. Cox and Ada Carter for their assistance in the design and construction of the experimental apparatus.

---

†Research sponsored by the U. S. Atomic Energy Commission under contract with Union Carbide Corporation.

[1]G. J. Schulz, Phys. Rev. 112, 150 (1958).

[2]G. J. Schulz, Phys. Rev. 116, 1141 (1959).

[3]R. K. Curran, J. Chem. Phys. 38, 780 (1963).

[4]J. C. Y. Chen, in Advances in Radiation Chemistry (John Wiley & Sons, Inc., New York, 1968), Vol. I.

[5]D. Rapp, T. E. Sharp, and D. D. Briglia, Phys. Rev. Letters 14, 533 (1965).

[6]G. J. Schulz and R. K. Asundi, Phys. Rev. 158, 25 (1967).

[7]R. N. Compton and L. G. Christophorou, Phys. Rev. 154, 110 (1967).

[8]T. E. Sharp and J. T. Dowell, J. Chem. Phys. 46, 1530 (1967).

[9]L. G. Christophorou, R. N. Compton, and H. W. Dickson, J. Chem. Phys. 48, 1949 (1968).

[10]W. L. Fite and R. T. Brackmann, in Proceedings of the Sixth International Conference on the Ionization Phenomena in Gases, Paris, 1963, edited by P. Hubert, E. Crêmieu-Alcan (S. E. R. M. A., Paris, 1964), Vol. I, p. 21; W. L. Fite, R. T. Brackmann, and W. R. Henderson, in Proceedings of the Fourth International Conference on the Physics of Electronic and Atomic Collisions (Science Bookcrafters, Hastings-on-Hudson, New York, 1965), p. 100.

[11]A. Skerbele and E. N. Lassettre, J. Chem. Phys. 42, 395 (1965).

[12]E. N. Lassettre, A. Skerbele, M. A. Dillon, and K. J. Ross, J. Chem. Phys. 48, 5066 (1968).

[13]M. M. Mann, A. Hustrulid, and J. T. Tate, Phys. Rev. 58, 340 (1940).

[14]K. Kraus, Z. Naturforsch. 16a, 1378 (1961).

[15]C. E. Melton, J. Chem. Phys. 45, 4414 (1966).

[16]T. E. Sharp and J. T. Dowell, J. Chem. Phys. (to be published).

[17]J. E. Collin, M. J. Hubin-Fromskin, and L. D'or, in Advances in Mass Spectrometry (Institute of Petroleum, London, 1968), Vol. 4, p. 713. (Proceedings of conference held in Berlin, 1967.)

[18]R. N. Compton, R. H. Huebner, P. W. Reinhardt, and L. G. Christophorou, J. Chem. Phys. 48, 901 (1968).

[19]L. G. Christophorou, R. N. Compton, G. S. Hurst, and P. W. Reinhardt, J. Chem. Phys. 43, 4273 (1965).

[20]H. H. Brongersma and L. J. Oosterhoff, Chem. Phys. Letters 1, 169 (1967).

[21]C. E. Kuyatt, J. A. Simpson, and S. R. Mielczarek, Phys. Rev. 138, 385 (1965).

[22]J. A. D. Stockdale, R. N. Compton, and P. W. Reinhardt, Phys. Rev. Letters 21, 664 (1968).

[23]G. Herzberg, Molecular Spectra and Molecular Structure (D. Van Nostrand Co., Inc., Princeton, New Jersey 1966), p. 609.

[24]G. J. Schulz, J. Chem. Phys. 33, 1661 (1960).

[25]A. Skerbele, M. A. Dillon, and E. N. Lassettre, J. Chem. Phys. 49, 5042 (1968).

[26]R. J. Thompson and A. B. F. Duncan, J. Chem. Phys. 14, 573 (1946).

[27]H. Sun and G. L. Weissler, J. Chem. Phys. 23, 1160 (1955).

[28]P. H. Metzger and G. R. Cook, J. Chem. Phys. 41, 642 (1964), report a single maximum near 800 Å (15.5 eV). This difference is probably due to the difficulties encountered with vacuum ultraviolet absorption studies.

[29]J. W. Otvos and D. P. Stevenson, J. Am. Chem. Soc. 78, 546 (1956).

[30]F. W. Lampe, F. H. Field, and J. L. Franklin, J. Am. Chem. Soc. 79, 6129 (1957).

[31]G. DeMaria, L. Malaspina, and V. Piacente, Ric.

Sci. A3, 681 (1963).

[32]For an authoritative review of the theory of dissociative electron attachment, see Ref. 4.

[33]D. Rapp and D. D. Briglia, J. Chem. Phys. 43, 1480 (1965).

[34]Due to the low ion currents at ~10 eV it was not possible to measure accurately the kinetic energies of the ions in this energy region by a retarding analysis similar to that performed on the ~6-eV peaks. The interesting suggestion[16] that NH_2^- from the 10-V peak is formed in a highly excited state therefore remains a possibility.

[35]For these particular measurements the effect of thermal motion of the molecule prior to attachment upon the dissociating particles in ion retardation measurements [P. J. Chantry and G. J. Schulz, Phys. Rev. 156, 134 (1967)] is approximately the same as the limits of error placed upon the determined dissociation energy (~0.15 eV).

PHYSICAL REVIEW VOLUME 180, NUMBER 1 5 APRIL 1969

Optical Potential for Li-HBr Collisions at Low Energies *

R. Marriott† and David A. Micha

Department of Physics and Institute for Pure and Applied Physical Sciences, University of California, San Diego, La Jolla, California 92037

(Received 9 December 1968)

A molecular optical potential has been used to reproduce the quenching of glory undulations in the total cross section of Li and HBr colliding at relative velocities 10^5 cm/sec $\leq v \leq 3.10^5$ cm/sec. The experimental results over the whole velocity range are well fitted by a r^{-12} law for the imaginary part of the potential. Complex phase shifts, opacity function, and elastic angular distribution have been calculated with this potential. Comparison with calculations using a real potential shows rainbow and supernumerary rainbow maxima and an increase of intensities at large angles in both cases. The main effect of inelastic transitions is to decrease the scattering intensity at large center of mass angles.

I. INTRODUCTION

We present in this contribution results on a molecular optical potential which reproduces the quenching (i.e., decrease in the amplitude) of glory undulations observed recently[1] in the total cross section of Li and HBr colliding in the range of relative velocities 10^5 cm/sec $\leq v \leq 3.10^5$ cm/sec, or relative kinetic energies from 0.033 to 0.301 eV. Glory undulations were predicted[2] and measured[3] some time ago for atom-atom collisions and their origin is well understood. More recently, measurements made with crossed beams of atoms and molecules indicate a quenching of these glory undulations that can in general be attributed to excitation of vibration-rotation levels of the molecule and to reaction.[4-7]

II. OPTICAL POTENTIAL FOR Li+HBr

In the case of Li + HBr at the relative kinetic energies investigated, excitation of vibrational levels is forbidden by energy conservation. Contribution of reactions in the region of impact parameters relevant to the glory effect is expected to be small.[1,6] The quenching may then be attributed to rotational excitation of HBr. This is interpreted here as equivalent to absorption of the scattering flux, and may be discussed in terms of optical (complex) molecular potentials.[8] Such a potential, taken as

$$U(r) = V(r) - i\,W(r) \tag{1}$$

was used to solve a system of two radial equations for the scattering function $y(r)$, with asymptotic form

$$y(r) \sim kr\{j_l(kr) + t_l(k)[n_l(kr) + i j_l(kr)]\}, \tag{2}$$

$$t_l(k) = (2i)^{-1}[\exp(2i\eta_l) - 1], \tag{3}$$

$$\eta_l = \xi_l + i\zeta_l, \tag{4}$$

where r is the interparticle distance, k the relative wave number, and j_l and n_l first- and second-class spherical Bessel functions. The equations